# CHAPTER ONE HUNDRED TWENTY SEVEN

## LONGSHORE VARIABILITY OF WAVE RUN-UP ON NATURAL BEACHES

R. A. Holman* and A. H. Sallenger, Jr.**

ABSTRACT

The longshore variability of wave run-up from a natural beach is examined using data from a large field experiment at the Field Research Facility in Duck, North Carolina, in October, 1982. Two particular runs were selected for intensive analysis. These were chosen to represent a dissipative and a reflective surf zone condition, so have Iribarren numbers 0.97 and 1.81 respectively. The dissipative data run showed much more uniform statistics in the longshore than did the reflective run. Also, the dissipative run was dominated by the infragravity band energy while the reflective run was dominated by the incident band. Selection of several important frequency bands for frequency-domain EOF analysis showed that the lower frequency peaks appeared to be associated with leaky modes (very long longshore wavelengths) and the pier had little influence. On the other hand, higher frequencies were clearly influenced by the pier in both amplitude and phase. An interesting subharmonic peak from the reflective run appeared to be a low (but not zero) mode standing edge wave.

A new technique,time exposure photography, is introduced. It allows the quick determination of longshore variability such as would be produced by a dominant standing edge wave. It can also be used to image offshore bathymetry and sand bar systems.

## INTRODUCTION

Wave run-up, the time-varying motion of the water's edge relative to still water level, is generally considered composed of two components, the set-up and the swash. If we denote the time series of run-up as $\eta_R(t)$, then

$$\eta_R(t) = \overline{\eta} + R(t),$$

where $\overline{\eta}$, the time average of the time series, is the set-up and

* Associate Professor, College of Oceanography, Oregon State University, Corvallis, OR, 97331.
**United States Geological Survey, Menlo Park, CA, 94025.

R(t) is the swash. Both of these quantities are of considerable interest to engineers. The combination of set-up and swash must be considered for the determination of safe set-back distances for structures on a coast. The velocities of the swash may provide the major erosive force on sediment or artificial structures.

While run-up at a point is a useful quantity to measure, it is longshore gradients of run-up which provide clues to some of the most interesting nearshore dynamics. Bowen (1969) showed how longshore gradients in set-up would force longshore currents, and so could generate rip currents at set-up minima. For the swash, it is the longshore phase relations which are most useful in that they can be used to define a longshore wavenumber, $k_y$, of the motion. This is particularly relevent to the understanding of the infragravity band in nearshore wave spectra (frequencies from 0.003 to 0.05 Hz). There has been a great deal of recent debate whether these long period motions are in the form of discrete free waves trapped to the shoreline, called edge waves, or alternately in non-trapped waves called leaky modes. For a particular frequency, $\sigma$, these possibilities are distinguished by

$$\sigma^2 \leq gk_y \text{ - edge waves}$$
$$\sigma^2 \geq gk_y \text{ - leaky modes.}$$

The wave for which the equality holds is called the cutoff mode. Thus measurement of the longshore structure, hence longshore wavenumber, of the motions is the most direct way to resolve the controversy.

It is the intention of this paper to examine the longshore variability of run-up from a natural beach based on an extensive dataset obtained at Duck, North Carolina in October, 1982. We will first describe the general experimental layout and the field techniques used. Two runs, representing very different incident wave conditions, are then selected for intensive study. These data are analyzed both in terms of their general statistics and in terms of frequency through frequency-domain EOF analysis. In the final section we present a new technique, time-exposure photography, to quickly describe longshore variability in swash statistics. The technique also has application to the remote sensing of offshore bathymetry.

## THE FIELD EXPERIMENT

In October 1982 a large field experiment was carried out at the CERC Field Research Facility (FRF) at Duck, North Carolina (Mason et al, in press). The FRF is located in the middle of 100 km stretch of barrier islands with the only topographic perturbation in the longshore being the pier itself which extends 560 m offshore and causes some interuption of the natural contours (Miller et al, 1983). The average beach face slope was approximately 1:10 although this value varied significantly through the experiment and on several

occasions (when the shoreline was very rhythmic) in the longshore. A bar system was present approximately 50 m offshore although the position and amplitude of the bar varied in response to storms. Bar morphology varied from linear to crescentic. A typical example of moryhology in the vicinity of the pier is shown in Figure 1.

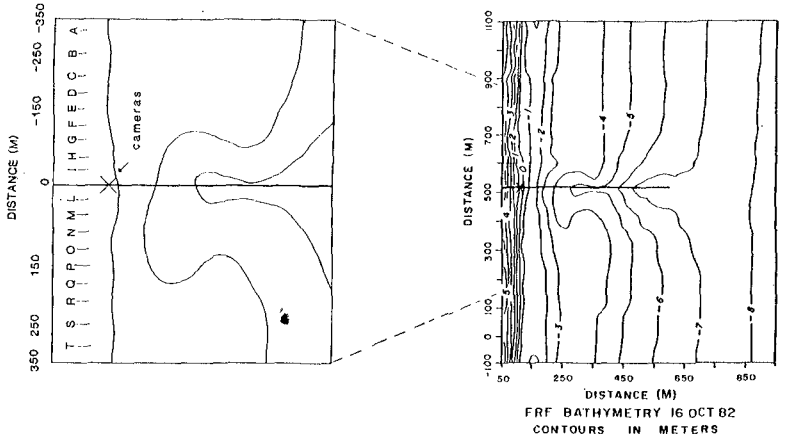


Figure 1. Typical bathymetry in the environment of the pier for October, 1982 (right hand figure). On the left is a blow-up of teh beach immediately surrounding the pier, showing the longshore locations of ranges referred to later.

Run-up data were collected using longshore-looking time-lapse photography from super 8 movie cameras mounted on scaffolding on the pier, approximately 13 m above mean sea level. Large markers were placed in pairs, spaced 10m in the cross-shore direction, every 50 m down the beach for 300 m on either side of the pier. Additional single markers were placed at odd multiples of 25 m. The markers served as a reference for the beach profile grid and provided scale for the film images.

A data run usually consisted of running two movie cameras synchronously, one pointed to the north and one to the south. A frame was shot every second for a total run length of 35 min, or 2100 frames. Slight differences in the digitizing interval were corrected by carefully timing the length of each run, counting the number of frames taken, and calculating the average $\Delta t$. Laboratory studies have shown no noticeable drift in this number through a 35 min period.

Digitization of the film data for any of the longshore locations is accomplished with a computer-assisted digitization scheme described in Holman and Guza, 1984. Replicate digitizations by different operators , performed on a number of films, showed the standard deviation on set-up and significant swash height measurements presented here to be approximately 10%. Inter-calibration of the film technique with the dual resistance wire runup sensor on a low-slope beach showed some systematic differences in measured means and standard deviations, with the film technique registering a slightly higher mean, and a 35% larger standard deviation (83% larger variance) than the wire sensor (Holman and Guza, 1984) . This is partly related to the sensitivity of the wire sensor to the height of the wire above the beach, and partly to the subjective interpretation of rundown of the films.

Beach surveys were carried out using the FRF Zeiss Elta-2 electronic total station system. This gives profile data, corrected to mean sea level, with an accuracy of better than 0.5 cm over the area of filming. These data were used to transform the raw cross-slope runup data to a vertical signal. All data presented in this paper will be in terms of the vertical component of runup. The profile data were also used to define a foreshore beach slope, $\beta$, as the mean slope over the 5m width of beach surrounding the mean sea level at the time of the run. Profile data were collected at least every two days and up to twice per day when the profiles were changing rapidly.

Incident wave data were collected from a waverider buoy positioned 3 km offshore in approximately 20 m depth. Incident significant wave height is calculated as $H_0 = 4\sigma$, where $\sigma$ is the standard deviation of a twenty minute time series. Incident period is the period associated with the peak energy in the spectrum. Tide data is provided by a NOAA tide gauge attached to the end of the pier. Raw tide gauge data, consisting of spot measurements of sea surface elevation every six minutes, showed a standard deviation of 0.04 m during storms. Mean sea level was estimated from the average of the 6 consecutive measurements corresponding to the data run. The tide gauge was outside the surf zone for all but the largest storms.

## OBSERVATIONS

Figure 2 shows the incident wave height and period statistics for the month of October, 1982, and indicates the duration of the experiment. Through the three weeks of the experiment, more than 80 films were exposed. Given the wealth of data available, it was decided to select two particular runs for intensive analysis for this paper. The two runs chosen were picked to represent different sorts of surf zone conditions. Run 19, shown in figure 2 as occuring near the beginning of the first major storm, is representative of dissipative conditions, with a wide surf zone of spilling breakers.

The deep-water incident wave height was 2.4 m with a peak period of 12 seconds. The longshore average beach slope was 0.10. By contrast, run 56 represents fairly reflective surf zone conditions. The incident wave height was 0.7 m, period 12.5 seconds, and average beach face slope 0.10.

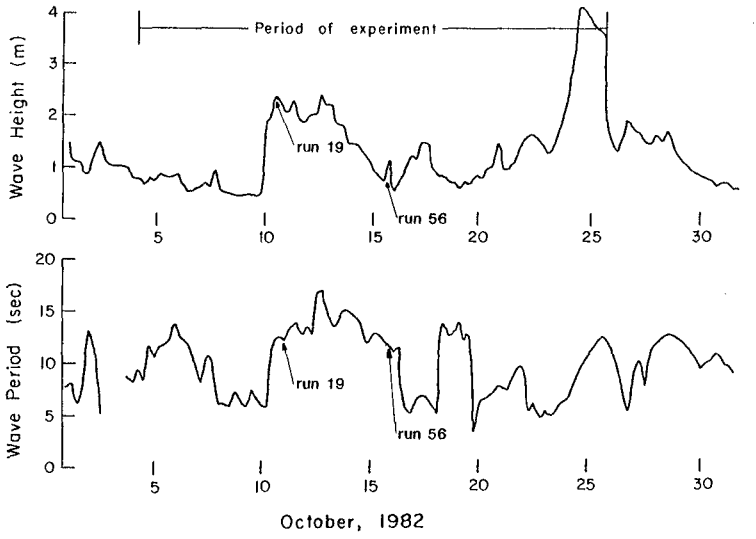


Figure 2. Significant wave height and peak period measured at the offshore waverider in 20 m depth. Noted are the duration of the entire experiment and the times of the two runs selected for intensive analysis.

Several non-dimensional measures exist which express the degree to which a surf zone is dissipative or reflective. One of these, the Iribarren number $\xi_0$, is given by

$$\xi_0 = \frac{\beta}{(H_0/L_0)^{1/2}}$$

where $H_0$ is the deepwater significant wave height and $L_0$ the deepwater wavelength associated with the peak period in the incident spectrum. For run 19 the Iribarren number was 0.97, while for run 56 it was 1.81. Previous papers had shown that $\xi_0$ or a similar parameter is an important parameter in swash dynamics (Guza and Inman, 1975; Holman and Sallenger, in press). Thus it is of interest

to look for systematic differences between these two data runs.

Figure 3 shows the significant swash height and the set-up statistics for runs 19 and 56 as a function of longshore distance. Several general observations can be made from these figures. The first is regarding the influence of the FRF pier, located at y=0. For run 19 there are systematic differences in both these quantities across the pier with the significant swash height changing from 1.49±0.13 (error bars being one standard deviation) to the north of the pier to 2.01±0.22 to the south, and set-up changing from 1.24%0.18 to the north to 0.80%0.14 to the south. Interestingly, the incident waves approached from 20° north of the local beach normal, so the higher swash was actually in what should have been a shadow zone. We can only speculate that this arises from refraction over the complicated bathymety associated with the pier.

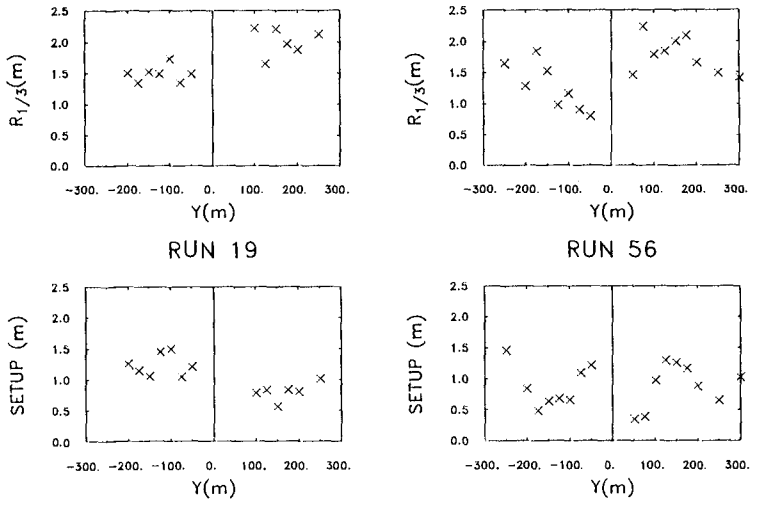


Figure 3. Significant swash height and set-up statistics for runs 19 and 56 as a function of longshore distance. The solid line at y=0 is the FRF pier.

For run 56 the swash height varies from 1.27±0.37 north of the pier to 1.78±0.30 to the south. Again the larger swash is to the south despite an angle of incidence 8° to the north of local normal. The set-up data for this run show uniform statistics across the pier, from 0.89±0.34 to the north, to 0.89±0.36 to the south.

The second general observation regarding this figure is that if we consider the sides of the pier separately, the statistics associated with the dissipative conditions are a great deal more uniform in the longshore than those associated with the reflective conditions. The average standard error (standard deviation divided by the mean) for run 56 was 31.1%, about 2.4 times the value, 13.1%, for run 19. While one cannot make a conclusion about longshore uniformity based on two examples, the trend of reduced longshore variability during dissipative conditions has been noted by others including Wright and Short, 1983, and Garrow, 1985. Note that a small longshore variability in bulk statistics does not indicate that longshore dependent processes such as edge waves are not operating, just that their statistics vary little when averaged through all frequencies. The frequency dependency of these data will be examined in the next section of the paper.

The final point to note regarding figure 3 is that despite a large difference in the incident wave height between these two runs (2.4 versus 0.7m), the set-up and swash statistics are not strongly different. In other words, the relative set-up and swash (normalized by the incident wave height) for the high Irribarren number day is much larger than for the low Iribarren number day. This dependence of non-dimensional run-up statistics on Iribarren number was noted also in Holman and Sallenger, in press (not surprisingly, since that paper was based on the same dataset).

## FREQUENCY-DEPENDENT ANALYSIS

To understand the longshore variability of statistics in greater detail, it was necessary to resolve the data into the frequency domain and perform frequency-dependent analysis. Figures 4 and 5 show the spectra for each longshore range for runs 19 and 56, respectively. Spectra for individual ranges are plotted according to the indicated axes but are each displaced vertically 0.615 orders of magnitude from the previous. Spectra labels correspond to the longshore locations shown in figure 1. Also shown are the frequency bands, labelled at the bottom of the figure, which will be used for subsequent frequency-domain EOF analysis. These frequency bands are 0.005 Hz wide for the infragravity band (20 dof) and 0.01 Hz wide for higher frequencies (40 dof).

Systematic differences are evident between the spectra for the two days. For the reflective day, run 56, the single dominant peak is at the incident frequency and is just the standing wave component of the incident waves. For lower frequencies, the infragravity band is low energy and without significant structure. On the other hand, the spectra for the dissipative day, run 19, are dominated by the infragravity band. The spectral peak associated with the incident band, while still present, is of lower energy. There is also some structure through the infragravity band.

Analysis for each data run proceeded on a frequency band by frequency band basis. The results from only the three most important bands for each run will be presented in this paper. For run 19, band C (0.07-0.08 Hz) was taken to represent the incident waves. Band 8 (0.035-0.040 Hz) was selected since it appeared particularly energetic, especially in the north end of the array. Finally, band 4 (0.015-0.02 Hz) showed some signs of a significant peak, but, more

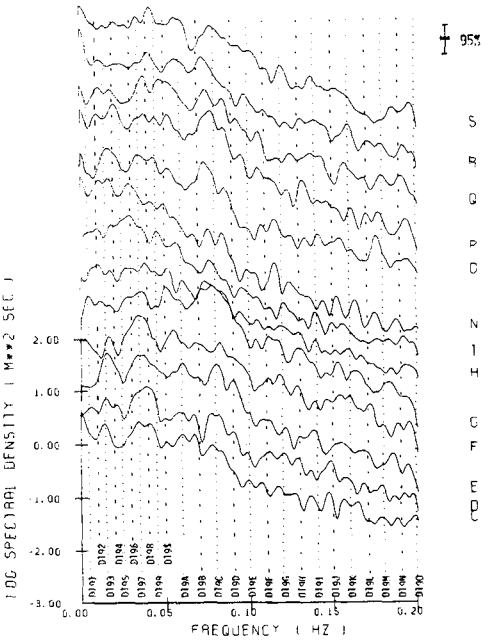


Figure 4. Displaced spectra for all longshore ranges digitized for run 19. Each spectrum is displace 0.625 orders-of-magnitude above the previous. Letters at right refer to longshore ranges indicated in figure 1, labels at bottom refer to individual frequency bands marked by the dotted lines (labels mark the upper limit of their band).

importantly, was found to be significant in data taken by offshore sensors described in this volume by Sallenger and Holman, in press. For the reflective day, run 56, the incident peak (band C, 0.07-0.08 Hz) was clearly important. Also common to all sensors was a low-frequency hill (band 1, 0.000-0.005 Hz). Finally, in a number of the spectra there are suggestions of a small peak at the

subharmonic frequency (band 8, 0.035-0.040 Hz, one half of the incident band frequency). Since Guza and Inman, 1975, have suggested the importance of the subharmonic on reflective beaches, further investigation of this band was indicated.

The longshore structure of each band was found using the technique of frequency-domain empirical orthogonal functions or EOFs (Wallace and Dickenson, 1972; Wang and Mooers, 1977; Holman and

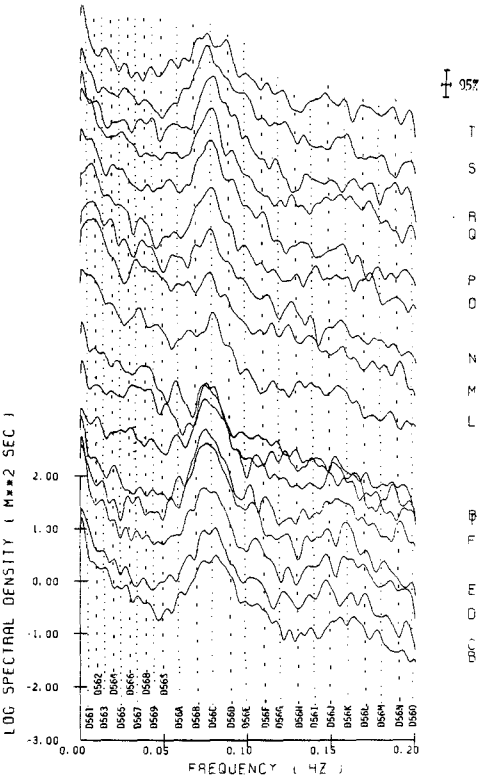


Figure 5. Same as figure 4, but for run 56.

Bowen, 1984). If the cross-spectra between pairs of ranges j and k for a particular frequency range is given by

$$U_{jk} = C_{jk} + iQ_{jk} \qquad j,k = 1,N$$

where C and Q are the cospectral and quadrature spectral estimates

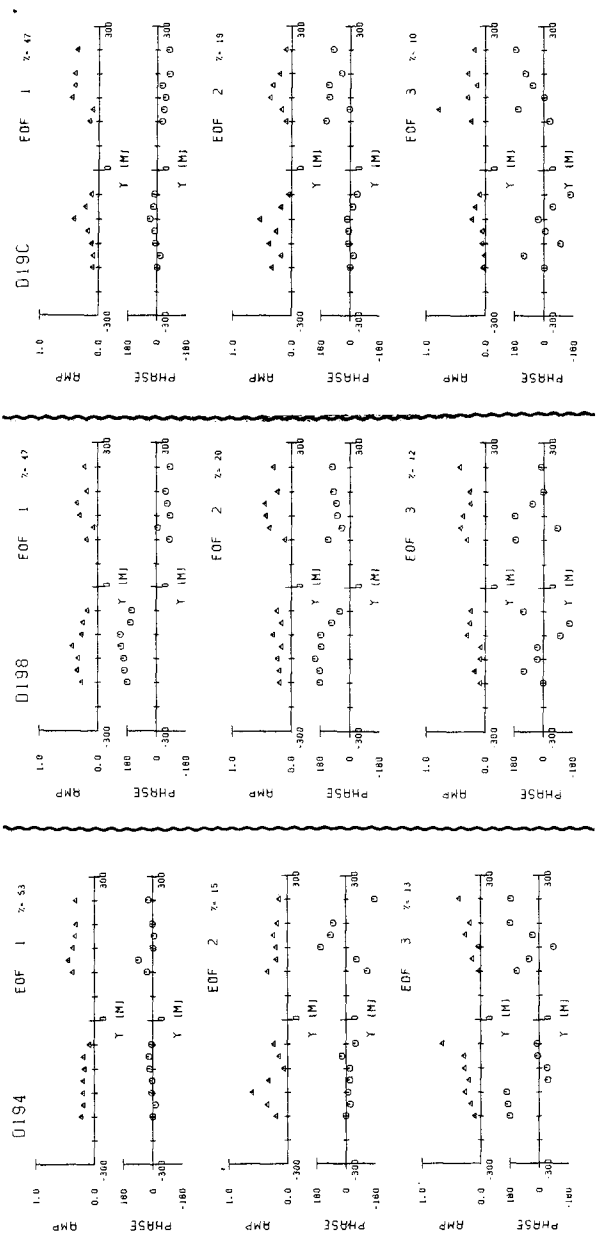


Figure 6. Frequency-domain EOFs for three dominant frequency bands for run 19. The band labels, at the top of each set of EOFs, correspond to figure 4. Band D194 is 0.015-0.020 Hz, band D198 is 0.035-0.040 Hz, and band D19C is the incident peak at 0.07-0.08 Hz. The amplitude and phase functions for the first three EOFs are slow in each case, along with the percent of the band variance explained by each.

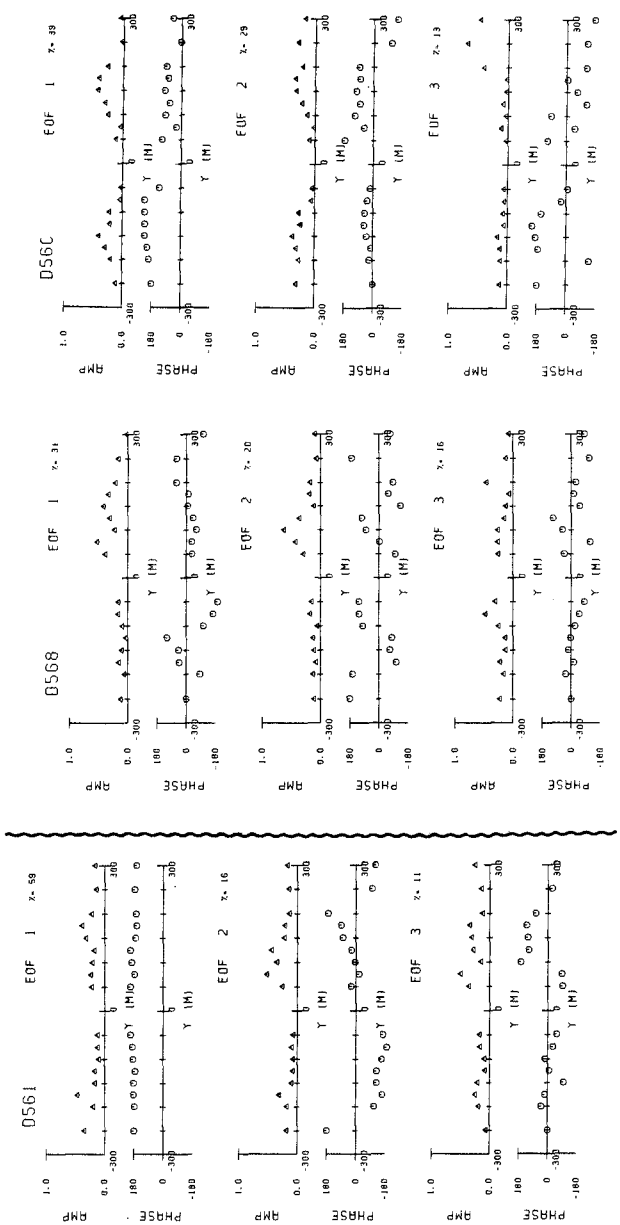


Figure 7. Same as figure 6 but for run 56. Band D561 is from 0.000-0.005 Hz, band D568 is 0.035-0.040 Hz, and band D56C is 0.07-0.08 Hz.

and N is the number of ranges, the EOFs are just the eigenvectors of $U_{ij}$. The eigenvectors will be complex, so can be expressed in terms of an amplitude and a phase. The amplitude is generally normalized to unit vector length and the phase expresses the relative phase amongst the ranges.

Figures 6 and 7 show the results of this analysis for the selected bands for runs 19 and 56 respectively. The first three EOFs, along with the percentages of the variance for the frequency band explained by each EOF, are shown in each case. We will examine each band in turn.

Band 4 of run 19 is dominated by the first EOF, with 53% of the variance being explained. The amplitude for this mode shows a definite change across the pier. However, the phase (with the exception of one point) is uniform alongshore. Thus the energy in this band is associated with a very small longshore wavenumber, possibly zero. The cutoff wavelength seperating the edge wave and leaky mode regimes is approximately 5 km for this band. For the 500 m length of this array this is equivalent to a 36° phase shift over the array length. While the present data cannot exclude the possibility that this is a very high mode edge wave, the phase information seems to indicate a leaky mode.

Band 8 of run 19 shows a rather more interesting picture. Again, the first mode dominates with 47% of the variance. For this mode, the amplitude shows more variability. Moreover, the phase shows a dramatic jump across the pier. A phase jump of 180° is suggestive of a wave standing in the longshore, possibly a standing edge wave. However, without indications of a second zero crossing away from the pier, the wavelength cannot be estimated and the edge wave hypothesis confirmed. Also it is interesting to note that if the pier, with its related pilings and bathymetry discontinuities, is thought to be a potential reflector of longshore-propogating wave motions, then the pier should be associated with a zero-crossing in longshore velocity, not in elevation.

Band C of run 19 represents the incident wave band. All EOFs indicate the localized effect of the pier on the wave amplitude. The phase of the first mode is relatively uniform although there is some indication that the wave arrives first near the pier (waves propogate "down-phase" in this analysis). This may be due to the greater water depths surrounding the pier. Note that there is no indication of southward progression expected from the 20° north angle of incidence.

Band 1 of run 56 corresponds to the very low frequency hill in most of the run 56 spectra. While there are some indications of variability in amplitude (the shoreface was also rhythmic), the phase of the first mode is uniform longshore. This is expected since these low frequencies are associated with long wavelengths. Since the wavelength of the cutoff edge wave is of the order of 62 km, these

Figure 8. Normal photograph of Short Sands Beach. Swash and breakers from such a snapshot give just one realization of dissipation in the swash or over a sand bar.

Figure 9. Ten-minute time exposure of the same scene taken immediately after Figure 8. Longshore variability of swash dissipation is obvious, but did not resproduce well from color slide.

data can say little to distinguish between edge waves and leaky modes at this frequency. However one can probably conclude that this mode is not a mode 0 or 1 edge wave, whose wavelengths would be less than a few kilometers.

Band 8 for run 56 represents the subharmonic band of the incident peak. Interestingly the energy contained in this band is much more evenly distributed among the EOFs. While the first EOF provides a somewhat confusing picture in phase, the second EOF is rather intriguing. The phase for this mode appears to make 180° phase jumps about every third point. This seems particularly apparent to the north of the pier (not in the shadow zone). This phase behaviour is consistent with a standing wave motion with a wavelength of 150 m. The wavelength of the cutoff mode for this band is 1100 m, so this motion lies clearly is the edge wave regime. While the appropriate beach slope for use in the edge wave dispersion relation is unclear, one can conclude that this motion is probably a standing edge wave of mode number that is low but greater than zero. This bears on the work of Guza and Davis, 1974, who predicted a mode zero edge wave based on theoretical and lab work.

Finally, band C of run 56 shows the incident wave behaviour. This band clearly shows the rather confusing effect of the pier on the incident waves. For all modes, the amplitude and phase show a strong variation away from the pier and on either side of the pier.

## TIME EXPOSURE PHOTOGRAPHY

The analysis of time series taken from different longshore locations reveals a great deal about the nature of wave motions in the nearshore. However it is often very difficult to collect suitable datasets, and the analysis can be somewhat long. An intriguing objective was to find a technique which could quickly show longshore variability in bulk wave statistics. Such a technique could resolve a dominant standing edge wave, for example,if one were present. A technique that does fill these needs is time-exposure photography. While a single snapshot provides only one realization of the wave field, a time exposure over a long period of time will average the image. For the case of waves in the nearshore the time exposure will be dominated by the white foam of breaking waves, so will essentially be an image of average breaking dissipation. The appropriate averaging time will depend on the time scales of variability. For normal incident waves, modulations generally occur on the time scale of minutes, so it was felt that a ten minute exposure would give an adequate averaging.

Figures 8 and 9 show an example of this technique. Figure 8 is a snapshot of an 800 m long bounded beach on the Oregon coast, Short Sands Beach. Individual wave breaking and run-up are easily distinguished. Figure 9 shows a ten minute time exposure of the same scene taken from the same vantage immediately following the snapshot.

The individual swashes now contribute to a broad white blur. Intriguingly, the width of this blur on the foreshore seems to vary in the longshore direction. Near the center of the beach the swash signal is its widest, while at points approximately 1/4 and 3/4 along the length of the beach, there are indications of a narrow swash zone. Beach surveys show little longshore variability, so the photographic signal appears to be the signature of a standing wave motion with two half-wavelengths trapped in the bay.

As a sidelight, it appears that this same technique can be used to effectively image offshore bathymetry. An offshore bar system is suggested by figure 8, but its structure is obscured by the complicated breaking pattern. However, in figure 9 the averaging of the time exposure has greatly simplified the apparent image of the bar system allowing one to easily distinguish the extent of the bar and the shoreward trough. The rather sharp delineation of the recommencment of breaking on the foreshore may indicate a step in the profile. It is apparent that this technique can be used to good advantage to map at least the general morphology and possibly, with further research, actual depths. The time exposure technique should be a very useful tool in the study of morphology changes during storms.

## CONCLUSIONS

This paper presents data on the longshore variability of wave run-up on natural beaches. From the simplest point of view this variability can be viewed as noise, showing uncertainty in run-up data collected at a single point. However it is through the phase relationships of this variability that a number of important questions can be answered about wave motions in the nearshore. The most important application is in the distinction between edge waves and leaky modes as the agents of fluid motion in the surf zone.

The longshore variability of swash was examined for two data runs selected from a much larger dataset collected at Duck, North Carolina, in October, 1982. The runs were selected as examples of dissipative and reflective surf zones. The data are all from within 300m of a pier.

The bulk run-up statistics of set-up and significant swash height were clearly influenced by the presence of the pier and its associated bathymetric discontinuities, being significantly different on either side of the pier. Interestingly, the swash height was higher on what should have been the shadow side of the pier, indicating odd refractive effects over the complex bathymetry. The longshore variability of these statistics was much larger for the reflective day (the higher Irribarren number).

Frequency-domain EOF analysis was used to examine the structure of three dominant energy peaks for each of the two data runs. This

analysis tended to reinforce the importance of the pier to phase and amplitude, although for low enough frequencies the dominant modes tended to show very long wavelengths, probably associated with leaky modes. An interesting peak at the subharmonic frequency of the reflective day appeared to be a standing edge wave with wavelength 150 m.

A new technique of time-exposure photography is shown capable of pointing out dominant variabilities in wave statistics such as would be associated with a standing edge wave. The technique also shows a great deal of promise for imaging offshore sand bar morphologies. Ease of logistics would allow the evolution of morphologies to be monitored through storms.

## ACKNOWLEDGEMENTS

Data collection for this paper was carried out under contract 12-08-0001-A-0022 from the U.S. Army Engineers Waterways Experiment Station, Coastal Engineering Research Center and the U.S. Geological Survey. The analysis work and development of the time exposure technique was supported by the Office of Naval Research, Coastal Sciences program under contract NR 388-168. Special thanks go to Aage Gribskov, Sara Culley and Eric Grann for help with the acquisition and digitization of the film data. Also, thanks to Harriet and her pals at the pier for donuts and other support.

## REFERENCES

Bowen, A. J. (1969). Rip currents. 1. Theoretical investigations. J. Geophys. Res., 74(23): 5467-5478.

Garrow, H. C. (1985). Shoreline rhythmicity on a natural beach. M.S. thesis, Oregon State University, pp189.

Guza, R. T. and R. E. Davis (1974). Excitation of edge waves by waves incident on a beach. J. Geophys. Res., 79(9): 1285-1291.

Guza, R. T. and D. L. Inman (1975). Edge waves and beach cusps. J. Geophys. Res., 80(21):2997-3012.

Holman, R. A. and A. J. Bowen (1984). Longshore structure of infragravity wave motions. J. Geophys. Res., 89(C4):6446-6452.

Holman, R. A. and A. H. Sallenger, Jr. (in press). Set-up and swash on a natural beach. J. Geophys. Res..

Mason, C., Sallenger, A. H., Jr., Holman, R. A., and W. A. Birkemeier (1984). A comprehensive experiment on storm-related coastal processes. in Proc. 19th Conf. on Coastal Engineering, ASCE, in press.

Sallenger, A. H., Jr. and R. A. Holman (1984). Infragravity waves on a barred profile during a storm. in Proc. 19th Conf. on Coastal Engineering, in press.

Wallace. J. M. and R. E. Dickenson (1972). Empirical orthogonal representation of time series in the frequency domain, I, Theoretical considerations. J. Appl. Meteorol., 11:887-892.

Wang, D. P. and C. N. K. Mooers (1977). Long coastal-trapped waves off the west coast of the United States, summer 1973. J. Phys. Oceanogr., 7:856-864.

Wright, L. D. and A. D. Short (1983). :Morphodynamics of beaches and surf zones in Australia. in CRC Handbook of Coastal Processes and Erosion,ed. P. D. Komar, CRC Press, Boca Raton, 35-64.